Journal of Organometallic Chemistry 696 (2011) 3169–3179

Contents lists available at ScienceDirect

Journal of Organometallic Chemistry

journal homepage: www.elsevier.com/locate/jorganchem

Cyclometalated complexes derived from calix[4]arene bisphosphites and their catalytic applications in cross-coupling reactions

Pathik Maji, Lepakshaiah Mahalakshmi, Setharampattu S. Krishnamurthy*, Munirathinam Nethaji

Department of Inorganic and Physical Chemistry, Indian Institute of Science, Bangalore 560012, India

ARTICLE INFO

Article history:
Received 29 March 2011
Received in revised form
23 June 2011
Accepted 23 June 2011

Keywords:
Calix[4]arene bisphosphites
Palladium and platinum dichloride complexes
Cyclometalation
Heck and Suzuki coupling reactions

ABSTRACT

Palladium and platinum dichloride complexes of a series of symmetrically and unsymmetrically substituted 25,26;27,28-dibridged *p-tert*-butyl-calix[4]arene bisphosphites in which two proximal phenolic oxygen atoms of *p-tert*-butyl- or *p*-H-calix[4]arene are connected to a P(OR) (R = substituted phenyl) moiety have been synthesized. The palladium dichloride complexes of calix[4]arene bisphosphites bearing sterically bulky aryl substituents undergo cyclometalation by C—C or C—H bond scission. An example of cycloplatinated complex is also reported. The complexes have been characterized by NMR spectroscopic and single crystal X-ray diffraction studies. During crystallization of the palladium dichloride complex of a symmetrically substituted calix[4]arene bisphosphite in dichloromethane, insertion of oxygen occurs into the Pd—P bond to give a P,O-coordinated palladium dichloride complex. The calix[4]arene framework in these bisphosphites and their metal complexes adopt distorted cone conformation; the cone conformation is more flattened in the metal complexes than in the free calix[4]arene bisphosphites. Some of these cyclometalated complexes proved to be active catalysts for Heck and Suzuki C—C cross-coupling reactions but, on an average, the yields are only modest.

1. Introduction

Calixarenes constitute an important class of synthetic macrocycles which display remarkable features such as conformational flexibility, presence of well-defined cavities, and ability to undergo modifications at both upper and lower rims. Calixarene chemistry has grown along several directions in recent years [1,2]. Particularly striking are the developments in the transition metal chemistry of phosphorus(III) functionalized calix[4]arenes [3–9] and the use of these phospha—calixarene ligands in catalysis [2a,3b,4d,4j,6b,7,8d]. A previous study in our laboratory has shown that the palladium dichloride complex of *p-tert*-butyl-calix[4]arene bisphosphite $\mathbf{L}^1$ readily undergoes cyclometalation by C—C bond scission to give a palladacycle [5a]. In this paper, we elaborate on this theme by reporting the synthesis of cyclometalated complexes derived from palladium and platinum dichloride complexes of a series of symmetrically substituted calix[4]arene bisphosphites ($\mathbf{L}^2$—$\mathbf{L}^6$) and the unsymmetrically substituted calix[4]arene bisphosphites ($\mathbf{L}^7$—$\mathbf{L}^9$) [10] (Chart 1). In view of the current interest in palladacycles as active catalysts for C—C bond-forming reactions [11,12], we also present here our preliminary results on the use of the cyclometalated complexes of calix[4]arene bisphosphites as catalysts for Suzuki- and Heck-type cross-coupling reactions. The utility of bisphosphites of the type $\mathbf{L}^1$—$\mathbf{L}^6$ in rhodium-catalyzed hydroformylation reactions has been reported by Paciello et al [7].

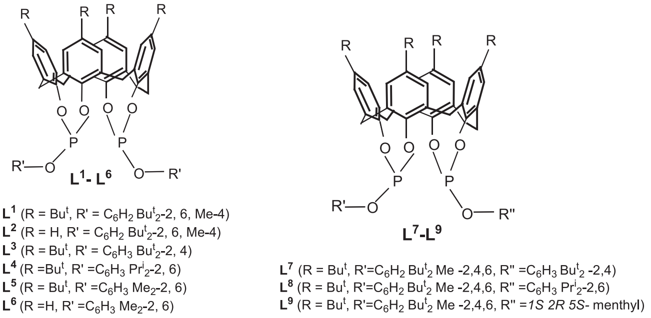

$\mathbf{L}^1$ (R = Bu^t, R' = $C_6H_2\,Bu^t{}_2$-2, 6, Me-4)
$\mathbf{L}^2$ (R = H, R' = $C_6H_2\,Bu^t{}_2$-2, 6, Me-4)
$\mathbf{L}^3$ (R = Bu^t, R' = $C_6H_3\,Bu^t{}_2$-2, 4)
$\mathbf{L}^4$ (R =Bu^t, R' =$C_6H_3\,Pr^i{}_2$-2, 6)
$\mathbf{L}^5$ (R = Bu^t, R' =$C_6H_3\,Me_2$-2, 6)
$\mathbf{L}^6$ (R =H, R' =$C_6H_3\,Me_2$-2, 6)

$\mathbf{L}^7$ (R = Bu^t, R'=$C_6H_2\,Bu^t{}_2$ Me -2,4,6, R'' =$C_6H_3\,Bu^t{}_2$ -2,4)
$\mathbf{L}^8$ (R = Bu^t, R'=$C_6H_2\,Bu^t{}_2$ Me -2,4,6, R'' =$C_6H_3\,Pr^i{}_2$-2,6)
$\mathbf{L}^9$ (R = Bu^t, R'=$C_6H_2\,Bu^t{}_2$ Me -2,4,6, R'' =*1S 2R 5S*- menthyl)

Chart 1.

---

* Corresponding author. Tel.: +91 80 2293 2401; fax: +91 80 2360 0683.
E-mail address: sskrish@ipc.iisc.ernet.in (S.S. Krishnamurthy).

0022-328X/$ – see front matter © 2011 Elsevier B.V. All rights reserved.
doi:10.1016/j.jorganchem.2011.06.027

2. Results and discussion

2.1. Palladium and platinum complexes of symmetrically and unsymmetrically substituted calix[4]arene bisphosphites

The symmetrically substituted calix[4]arene bisphosphites $\mathbf{L}^2$–$\mathbf{L}^5$ react with 1 M equivalent of $PdCl_2(PhCN)_2$ or $PdCl_2(COD)$ in toluene at 75 °C to give the complexes **2**, **3a**, **4** and **5** respectively which are isolated as pale yellow solids. The analogous dichloro platinum complex **3b** is isolated as a colourless solid from the reaction of $PtCl_2(COD)$ with the symmetrically substituted calix[4]arene bisphosphite $\mathbf{L}^3$.The symmetrically substituted calix[4]arene bisphosphite $\mathbf{L}^6$ forms the dichloro palladium complex **6** at room temperature. Similarly, the dichloro palladium complexes **11**–**13** are synthesized from the unsymmetrically substituted bisphosphites $\mathbf{L}^7$–$\mathbf{L}^9$. The dichloro palladium complexes **2**, **3a**, **11** and **12** and the dichloro platinum complex **3b** are transformed into the corresponding cyclometalated complexes **8**, **9a**, **9b**, **14** and **15** when heated in toluene at 95 °C. These cyclometalated complexes are also obtained directly from the reaction of $PdCl_2(PhCN)_2$ or $PtCl_2(COD)$ with the respective calix[4]arene bisphosphite at 95 °C. The dichloro palladium complexes **4** and **13** do not undergo cyclometalation reaction when heated at or above 95 °C. The reaction mixture turned black indicating the decomposition of the complex to palladium metal. The above reactions are shown in Scheme 1 (for symmetrically substituted bisphosphites) and Schemes 2 and 3 (for unsymmetrically substituted bisphosphites). The calixarene bisphosphite $\mathbf{L}^1$, its palladium dichloride complex **1** and the corresponding cyclopalladated complex **7** previously reported from our laboratory [5a] are also included in Scheme 1 for comparison.

The cyclometalated complexes **9a**, **9b** and **14** are formed by C–H bond activation whereas the formation of the cyclometalated complexes **8** and **15** must involve the loss of a *tert*-butyl group prior to C–H activation as noted previously for complex **7** [5a].

During crystallization of the palladium dichloride complex **1** in dichloromethane, insertion of oxygen occurs into the P–Pd bond to give the P,O-coordinated palladium dichloride complex **10** (Scheme 4). The structure of complex **10** has been established by X-ray crystallography (see below). Mahalakshmi [13] had noted that the oxidation of the bisphosphite $\mathbf{L}^1$ to the corresponding bisphosphate by treatment with hydrogen peroxide was difficult but the oxidation occurred readily with palladium acetate in dichloromethane in the presence of atmospheric air to give the corresponding bisphosphate. Presumably, the oxidation proceeds via the complex **10**.

The ^{31}P NMR data for the symmetrically substituted calix[4]arene bisphosphites ($\mathbf{L}^1$–$\mathbf{L}^6$) and their palladium and platinum

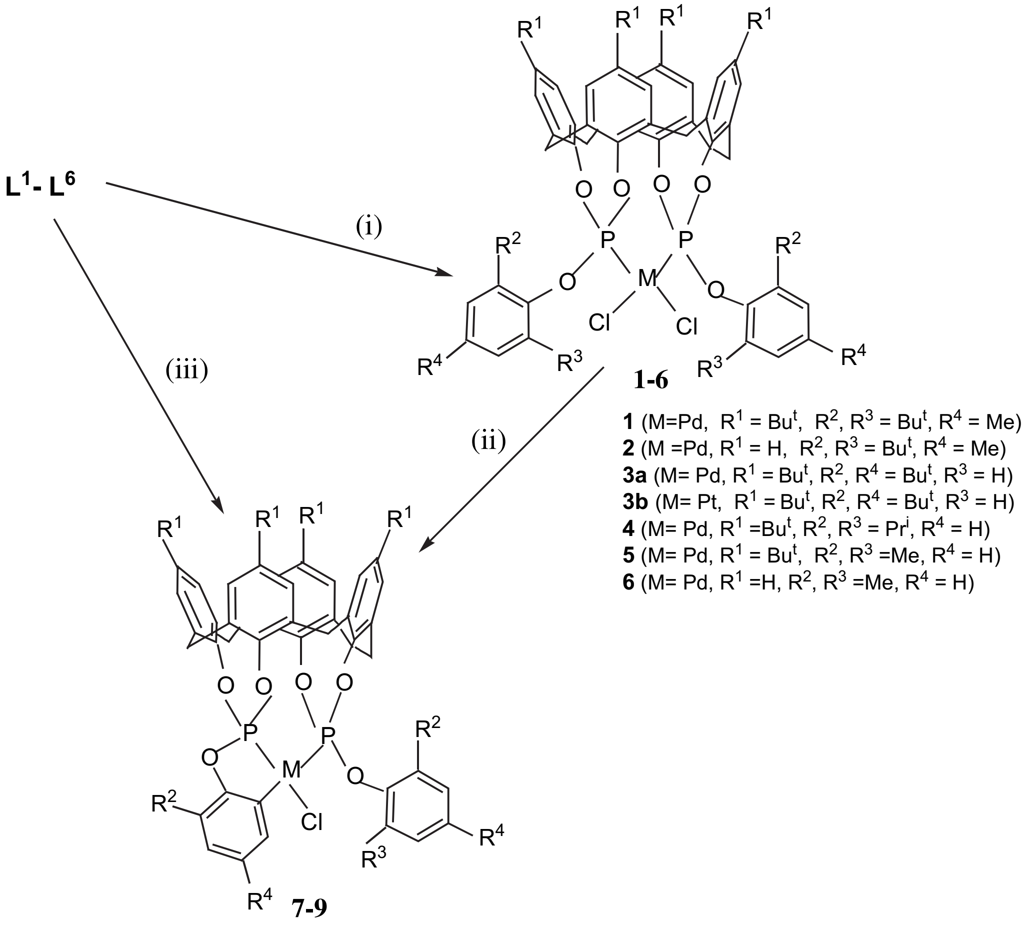

1-6

1 (M=Pd, R^1 = Bu^t, R^2, R^3 = Bu^t, R^4 = Me)
2 (M =Pd, R^1 = H, R^2, R^3 = Bu^t, R^4 = Me)
3a (M= Pd, R^1 = Bu^t, R^2, R^4 = Bu^t, R^3 = H)
3b (M= Pt, R^1 = Bu^t, R^2, R^4 = Bu^t, R^3 = H)
4 (M= Pd, R^1 =Bu^t, R^2, R^3 = Pr^i, R^4 = H)
5 (M= Pd, R^1 = Bu^t, R^2, R^3 =Me, R^4 = H)
6 (M= Pd, R^1 =H, R^2, R^3 =Me, R^4 = H)

7-9

7 (M=Pd, R^1 = Bu^t, R^2, R^3 = Bu^t, R^4 = Me)
8 (M=Pd, R^1 = H, R^2, R^3 = Bu^t, R^4 = Me)
9a (M =Pd, R^1 = Bu^t, R^2, R^4 = Bu^t, R^3 =H)
9b (M =Pt, R^1 = Bu^t, R^2, R^4 = Bu^t, R^3 = H)

Scheme 1. (i) $PdCl_2$ (COD) or $PtCl_2$ (COD) (ii) toluene, 95 °C, 24 h, (iii) $PdCl_2$ $(PhCN)_2$ or $PtCl_2$ (COD), toluene, 95 °C, 24 h.

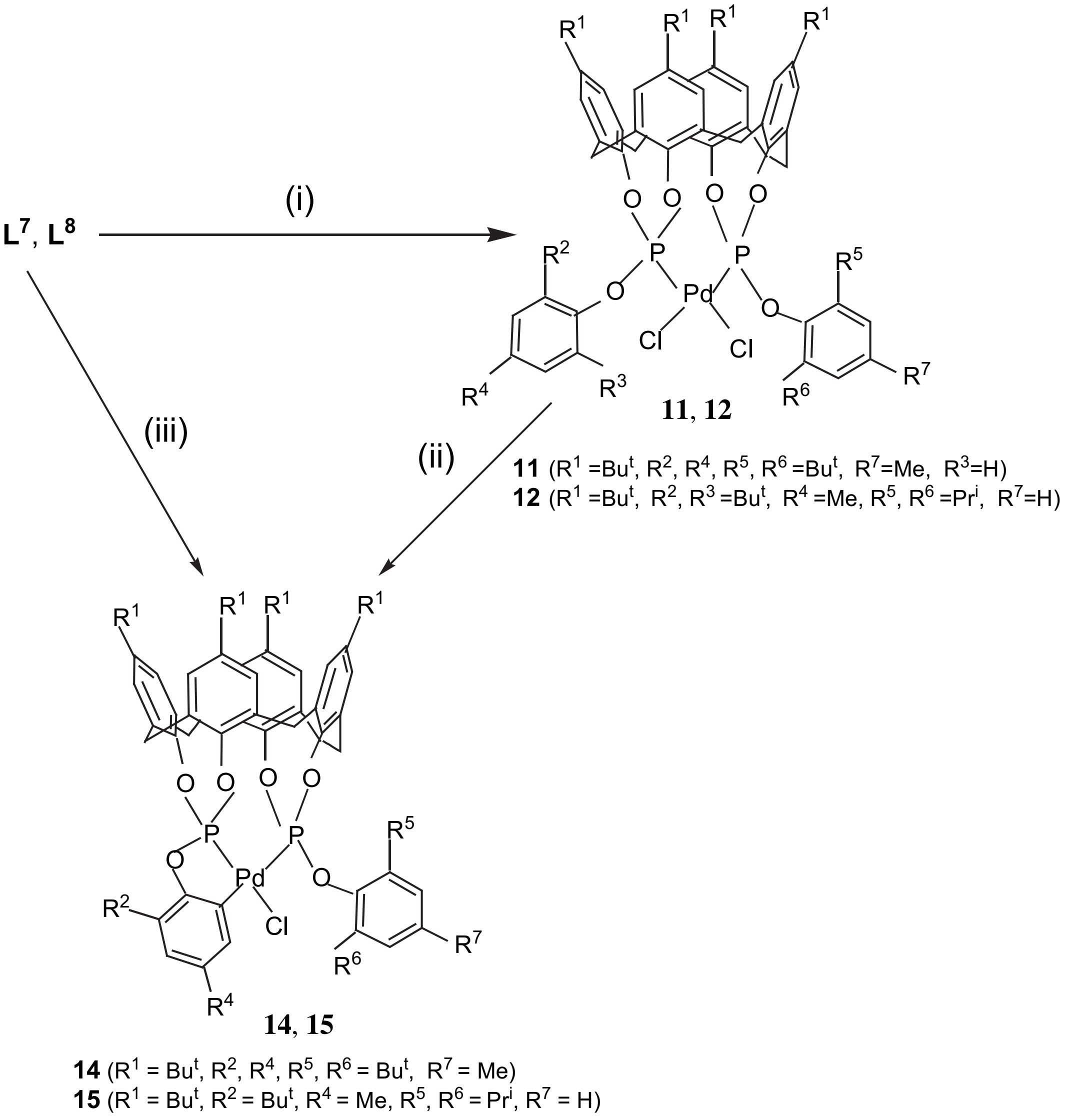

Scheme 2. (i) $PdCl_2$ (COD), toluene, 75 °C, 24 h, (ii) toluene, 95 °C, 24 h, (iii) $PdCl_2$ $(PhCN)_2$, toluene, 95 °C, 24 h.

complexes are listed in Table 1. The data for the unsymmetrically substituted calix[4]arene bisphosphites ($\mathbf{L}^7$–$\mathbf{L}^9$) and their palladium complexes are given in Table 2. The ^{31}P chemical shifts for the symmetrically substituted bisphosphite palladium dichloride complexes **1**, **2**, **3a**, **4**–**6** and the platinum dichloride complex **3b** lie very much upfield to those of the free ligands (see Table 1). The *cis* stereochemistry around the metal (Pd, Pt) centre is inferred from the far IR spectrum which shows two ν(M – Cl) bands in the range 312–328 cm^{-1} for each of the complexes. The ^{1}H NMR spectra of these palladium and platinum dichloride complexes display four doublets for the methylene protons of the calix[4]arene framework as observed for the corresponding bisphosphites (see Supplementary material).

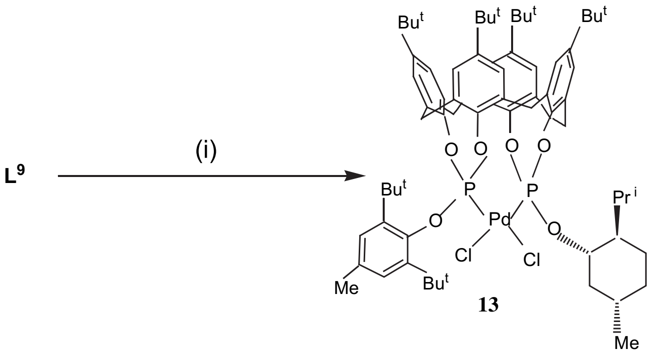

Scheme 3. (i) $PdCl_2$ (COD), toluene, 75 °C, 24 h.

The ^{31}P NMR spectra of palladium dichloride complexes (**11**–**13**) of unsymmetrically substituted calix[4]arene bisphosphites show an AB pattern. The spectrum of **13** is illustrated in Fig. S1 (see Supplementary material). For all the complexes, the downfield resonance (P_A) is assigned tentatively to P(O–C_6H_2–^{t}Bu$_2$–Me-2,4,6) group and the upfield resonance (P_B) to P(O–C_6H_3–^{t}Bu$_2$-2,4),P(O–$C_6H_3^i$Pr$_2$-2,6) or P(O-menthyl) group. These assignments are based on the ^{31}P chemical shifts for calix[4]arene bisphosphites and monophosphites containing various substituted phenyl groups [5a,e,10]. The ^{1}H NMR spectrum of each these palladium dichloride complexes (**11**–**13**) is similar to that of the respective calix[4]arene bisphosphite $\mathbf{L}^7$, $\mathbf{L}^8$ or $\mathbf{L}^9$.

The ^{31}P NMR spectra of the cyclometalated complexes **7**–**9**, **14** and **15** show an AX pattern. The ^{31}P NMR spectra of complexes **9a** and **9b** are shown in Fig. 1. The phosphorus chemical shifts for the

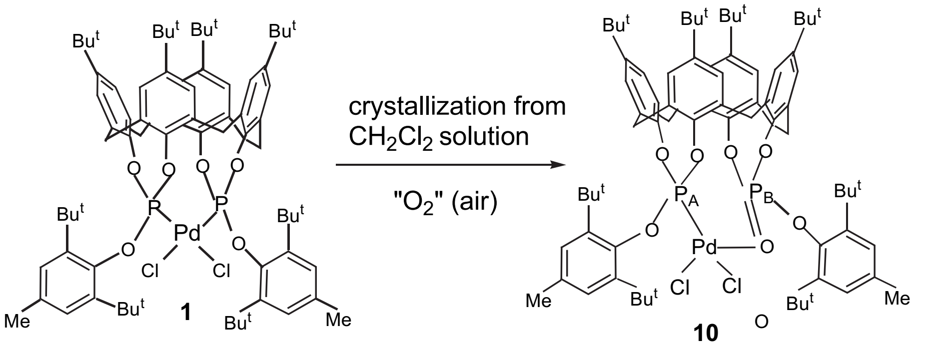

Scheme 4.

cyclometalated complexes **7**–**9** lie considerably downfield to those of the palladium and platinum dichloride complexes of symmetrically substituted bisphosphites (see Table 1). For the cyclopalladated complexes **8** and **9a**, the doublet in the downfield region is assigned to the phosphorus nucleus (P$_X$) which is *trans* to the coordinated aryl carbon atom; the doublet in the upfield region is assigned to the phosphorus nucleus (P$_A$) *cis* with respect to the coordinated aryl carbon atom. For cycloplatinated complex **9b**, the doublet (satellites ^{195}Pt, $^1J_{\text{Pt–P}} = 3390$ Hz) in the downfield region is assigned to the phosphorus atom (P$_X$) which is *trans* with respect to the coordinated aryl carbon atom. The other doublet (satellites ^{195}Pt, $^1J_{\text{Pt–P}} = 6496$ Hz) in the upfield region is assigned to the phosphorus atom (P$_A$) *cis* with respect to the coordinated aryl carbon atom. These assignments are based on the phosphorus chemical shift values for the methyl palladium chloro complexes of calix[4]arene bisphosphites [5e]. The ^{1}H NMR spectra of cyclometalated complexes show six doublets (three doublets in the downfield and other three doublets in the upfield region) with coupling constants typical of germinal protons. The formation of a 10-membered metallacycle in addition to the two eight membered rings containing phosphorus, is responsible for the nonequivalence of the methylene protons of the calix[4]arene framework [5a] (see Supplementary material for illustrative spectra).

The ^{31}P NMR spectrum of the palladium dichloride complex **10** shows two singlets at 74.4 (P$_A$) and −6.8 (P$_B$) ppm as the two phosphorus are in two different oxidation states (III and V) respectively. Because of the unsymmetrical nature, all the eight methylene protons of the calix[4]arene framework are nonequivalent (see Fig. S5 in Supplementary material).

2.2. *X-ray crystallographic studies*

The solid state structures of the symmetrically substituted bisphosphites **L**^{1}, **L**^{2} and **L**^{6}, the palladium dichloride complexes **4** and **10** and the cyclopalladated complexes **9a** and **14** have been determined by single crystal X-ray diffraction analysis. Details pertinent to data collection, structure solution and refinement are summarized in Table 3.

The ORTEP plots of the molecular structures of symmetrically substituted bisphosphites **L**^{1}, **L**^{2} and **L**^{6} are shown in Figs. 2–4 respectively. Selected bond lengths and angles are given in Table 4. The conformation of calix[4]arene backbone in these phosphites can be described in terms of relevant dihedral angles or torsion angles. The torsion angles involving the bridging methylene carbon atoms and aryl ring carbon atoms are listed in Supplementary material (Tables S1–S3). The torsion angles show the sequence of signs for ϕ and χ to be ±, ±, ±, ± for all bisphosphites as expected for cone conformation. However, the values of the torsion angles indicate that there is an appreciable deviation from the ideal cone conformation [$\phi = 90°$ and $\chi = -90°$] [14]. The distortion from the cone conformation is also reflected in the dihedral angles of the calix[4]arene aryl rings {A, B, C and D (for **L**^{1}; A = A′, B = B′)} with the plane X of the four methylene carbon atoms {C1, C2, C1′ and C2′ for **L**^{1} and C1, C8, C14 and C20 for **L**^{2} and **L**^{6}}, which are listed in Table 5. The distortion from ideal cone conformation in these bisphosphites is similar to that observed for calix[4]arene bisphosphites and monophosphites [5c,10].

The ORTEP plots of the molecular structures of palladium dichloride complexes (**4** and **10**) are shown in Figs. 5 and 6 respectively. Selected bond lengths and bond angles are given Table 6. The dihedral angles of the calix[4]arene aryl rings (A, B, C and D) with the plane X of the methylene carbon atoms (C2, C8, C14 and C20) are listed in Table 7. The torsion angles are listed in Supplementary material (Tables S4 and S5). The sequence of signs for the two torsion angles ϕ and χ confirms the cone conformation of calix[4]arene framework. In these two palladium dichloride complexes, the two aryl rings with larger torsion angles are parallel to each other; the other two aryl rings with smaller torsion angles

Table 1
The ^{31}P{^{1}H} NMR data for symmetrical bisphosphites (**L**^{1}–**L**^{6}) and transition metal complexes **1**–**9**.[a]

Symmetrical bisphosphites	δ	Dichloride complexes	δ	$\Delta\delta$	Cyclometallated complexes	δ	$^2J_{\text{P–P}}$ (Hz)
L^1	123.8	**1**	72.4	51.4	**7**	120.7(d) 103.6(d)	78.1
L^2	123.1	**2**	69.2	53.9	**8**	121.3(d) 101.6(d)	78.9
L^3	115.6	**3a**	72.9	46.9	**9a**	119.8(d) 106.9(d)	81.3
		3b	52.6	63.0	**9b**	114.2(d) ($^1J_{\text{Pt–P}} = 3390$ Hz), 94.8 (d) ($^1J_{\text{Pt–P}} = 6496$ Hz)	42.1
[b]**L**^{4}	119.8	**4**	71.5	48.3			
[b]**L**^{5}	118.8	**5**	70.7	48.1			
L^6	117.9	**6**	70.1	47.8			

[a] Recorded in CDCl$_3$ at 25 °C and at 161.9 MHz, δ in ppm, $\Delta\delta = (\delta_{\text{ligand}} - \delta_{\text{complex}})$ in ppm.
[b] Data from Ref. [10].

Table 2
The $^{31}P\{^1H\}$ NMR data for unsymmetrical bisphosphites ($\mathbf{L}^7$–$\mathbf{L}^9$) and transition metal complexes **11**–**15**.[a]

Unsymmetrical Bisphosphites[b]	δ		$^8J_{P-P}$ (Hz)	Dichloride complexes	δ		$^2J_{P-P}$ (Hz)	Cyclometallated complexes	δ		$^2J_{P-P}$ (Hz)
	P_A	P_B			P_A	P_B			P_A	P_B	
$\mathbf{L}^7$	123.2(d),	116.1(d)	243.1	**11**	73.0(d),	70.8(d)	71.3	**14**	121.4(d),	103.6(d)	78.9
$\mathbf{L}^8$	123.6(d),	119.3(d)	236.7	**12**	73.1(d),	70.7(d)	72.9	**15**	120.9(d),	106.3(d)	74.5
$\mathbf{L}^9$	126.6(d),	124.8(d)	223.8	**13**	81.3(bs),	70.3(d)	66.4				

[a] Recorded in $CDCl_3$ at 25 °C and at 161.9 MHz, δ in ppm.
[b] Data from Ref [10].

are tilted from the mean plane X of the methylene carbon atoms. This type of conformation is known as "flattened cone conformation" [14]. The O–P–O bond angles around phosphorus of the phosphate group in palladium dichloride complex **10** are larger than the O–P–O bond angles around the phosphorus of the phosphite group in the same complex **10** or complex **4**. The P–O bond distance (1.478 Å) of the phosphate group in which the oxygen is coordinated to palladium is longer than that observed for the corresponding *p-tert*-butyl-calix[4]arene bisphosphate ligand (1.448 Å) [13] whereas the other P–O bond distances are shorter.

The ORTEP plot of the molecular structure of the cyclopalladated complexes **9a** and **14** are shown in Figs. 7 and 8 respectively. Selected bond lengths and bond angles for complexes **9a** and **14** and the related cyclopalladated complex **7**, previously reported [5a] are listed in Table 8. The metrical data for the three cyclopalladated complexes **9a**, **14** and **7** are comparable. The calix[4]arene framework in the cyclopalladated complexes **9a**, **14** and **7** adopts a distorted cone conformation similar to that observed in the palladium dichloride complexes **4** and **10**. The distortion from cone conformation for complex **9a** is more than that observed for complexes **14** and **7** as can be inferred from the relevant dihedral angles (listed in Table 9) and torsion angles (see Supplementary material Tables S6 and S7 for complexes **9a** and **14** respectively). This is also reflected in the larger separation of the two opposite *para*-carbon atoms [C(11)–C(23)] in complexes **9a** and **14** (distance 10.09 Å and 9.67 Å respectively) compared to the analogous separation (9.44 Å) in complex **7** [5a].

The square planar coordination environment of the palladium atom in the complexes **4**, **10**, **7**, **9a** and **14** shows a pronounced tetrahedral distortion. This distortion is the largest for complex **4** (the $P_1Pd_1P_2/Cl_1Pd_1Cl_2$ dihedral angle 15.50°) and is the least for the complex **10** ($O_4Pd_1P_2/Cl_2Pd_1Cl_2$ 6.20°); the cyclopalladated complexes **9a**, **14** and **7** display intermediate level of distortion ($P_1Pd_1P_2/Cl_1Pd_1C_{34}$ 8.37°, $P_1Pd_1P_2/Cl_1Pd_1C_{34}$ 9.33° and $P_1Pd_1P_2/Cl_1Pd_1C_{36}$ 8.80° respectively). The tetrahedral distortion in complex **4** is higher than that (8.4–14.80°) observed in many palladacycles derived from sterically congested phosphites [15]. These data suggest that the relief of steric strain is the driving force for cyclometalation observed for the complexes **1**–**3**, **11** and **12**.

2.3. Palladium catalyzed Heck coupling reaction

The palladium catalyzed Heck coupling reaction between styrene and aryl halides (X = Br, I) was investigated using cyclopalladated complexes **7**, **8**, **9a** (derived from symmetrically substituted bisphosphites), **14** and **15** (derived from unsymmetrically substituted bisphosphites) as catalysts (see Scheme 5). In all the Heck reactions, only a single product (*trans*-stilbene) was obtained. The *cis* isomer or any other by-product was not formed as shown by thin layer chromatography and the ^1H NMR spectrum of the isolated product. The yields (%) of the product with different aryl halides and the turn-over-numbers (TONs) are shown in Table 10. The cyclopalladated complex **7**, which is derived from a sterically bulky *p-tert*-butyl bisphosphite $\mathbf{L}^1$, is the most effective catalyst among the cyclopalladated calix[4]arene bisphosphite complexes reported in this study. However, these cyclopalladated calix[4]arene bisphosphite complexes are less effective catalysts compared to other reported cyclopalladated complexes [16].

2.4. Palladium and platinum catalyzed Suzuki coupling reaction

Preliminary studies on Suzuki coupling reaction between phenyl boronic acid and aryl halides or substituted aryl halides (X = H, Me, OMe; Y = I, Br, Cl) in the presence of cyclopalladated complexes **7**, **8**,

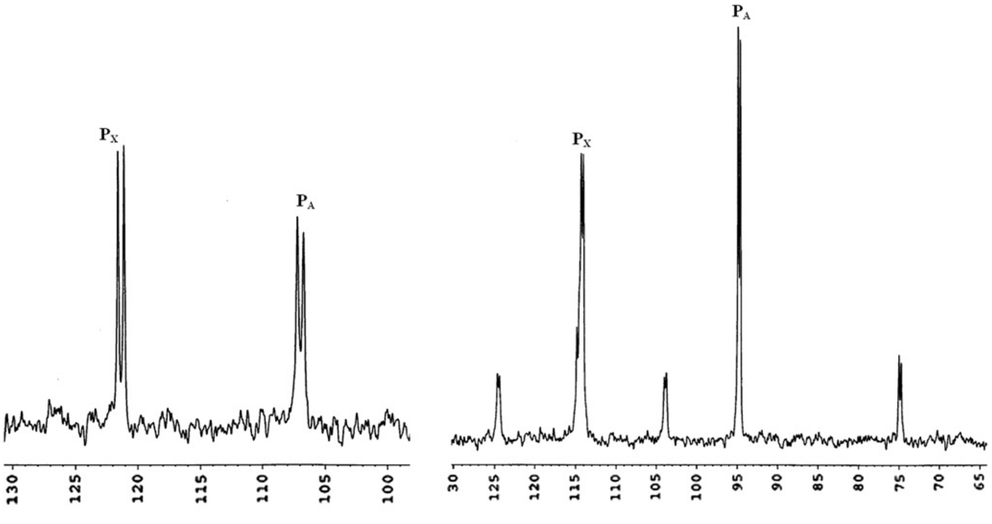

Complex **9a**

Complex **9b**

Fig. 1. The ^{31}P NMR spectra of cyclopalladated complex **9a** and cycloplatinated complex **9b** respectively.

Table 3

Crystal data for symmetrically substituted bisphosphites (**L**^{1}, **L**^{2}, **L**^{6}), palladium dichloride complexes **4**, **10** and cyclopalladated complexes **9a**, **14**.

Empirical formula	$C_{78}H_{120}O_{13}P_2$ (**L**^{1})	$C_{59}H_{68}Cl_2O_6P_2$ (**L**^{2})	$C_{44}H_{38}O_6P_2$ (**L**^{6})	$C_{68}H_{86}Cl_2O_6P_2$ Pd_1 (**4**)	$C_{74}H_{102}Cl_2O_9P_2Pd_1$ (**10**)	$C_{72}H_{93}Cl_1O_6P_2Pd_1$ (**9a**)	$C_{80}H_{107}Cl_1O_8P_2Pd_1$ (**14**)
Formula weight	1327.72	1005.97	724.68	1238.61	1374.80	1258.25	1400.45
Temperature	293(2) K	293(2) K	293(2) K	293(2) K	293(2) K	293(2) K	293(2) K
Wavelength	0.71070 Å	0.71073 Å	0.71073 Å	0.71073 Å	0.71073 Å	0.71073 Å	0.71073 Å
Crystal system	Monoclinic	Triclinic	Monoclinic	Monoclinic	Monoclinic	Trigonal	Monoclinic
Space group	*C*2/*c*	*P* − 1	*P*2/*n*	*C*2/*c*	*C*2/*c*	R-3	*P*2/*c*
Unit cell dimensions	$A = 23.551(5)$ Å $b = 17.508(7)$ Å $c = 19.299(5)$ Å $\alpha = \gamma = 90.00(2)^\circ$, $\beta = 102.35(2)^\circ$	$a = 12.411(5)$ Å $b = 13.624(6)$ Å $c = 18.195(8)$ Å $\alpha = 102.174(7)^\circ$, $\beta = 91.731(8)^\circ$, $\gamma = 111.907(7)^\circ$	$a = 13.374(2)$ Å $b = 18.593(3)$ Å $c = 14.827(2)$ Å $\alpha = \gamma = 90^\circ$, $\beta = 102.304(6)^\circ$	$a = 52.034(5)$ Å $b = 19.831(2)$ Å $c = 15.137(1)$ Å $\alpha = \gamma = 90.00^\circ$, $\beta = 105.655(2)^\circ$	$a = 24.406(7)$ Å $b = 17.723(5)$ Å $c = 39.158(1)$ Å $\alpha = \gamma = 90.00^\circ$, $\beta = 98.888(5)^\circ$	$a = 37.92(2)$ Å $b = 37.92(2)$ Å $c = 29.84(3)$ Å $\alpha = \gamma = 90.00^\circ$, $\beta = 120^\circ$	$a = 17.335(5)$ Å $b = 18.386(5)$ Å $c = 28.672(5)$ Å $\alpha = \gamma = 90.00^\circ$, $\beta = 106.84^\circ$
Volume	7774(4) Å^3	2770(2) Å^3	3602.2(10) Å^3	15040(2) Å^3	16735(8) Å^3	37147(6) Å^3	8746(4) Å^3
Z	4	2	4	8	8	18	4
Density (calculated)	1.102 Mg/m^3	1.206 Mg/m^3	1.336 Mg/m^3	1.094 Mg/m^3	1.091 Mg/m^3	1.102 Mg/m^3	1.064 Mg/m^3
Absorption coefficient	0.112 mm^{-1}	0.223 mm^{-1}	0.172 mm^{-1}	0.402 mm^{-1}	0.370 mm^{-1}	0.336 mm^{-1}	0.325 mm^{-1}
F (000)	2768	1068	1520	5216	5824	11988	2976
Crystal size (mm)	0.14 × 0.08 × 0.12	0.38 × 0.32 × 0.28	0.46 × 0.38 × 0.32	0.48 × 0.38 × 0.03	0.56 × 0.42 × 0.36	0.42 × 0.36 × 0.28	0.64 × 0.32 × 0.24
Theta range for data collection	1.70–24.97°	1.66–26.50°	2.50–26.50°	1.59–24.71°	1.43–25°	2.50–27.50°	2.50–27°
Index ranges	$0 \le h \le 27$ $0 \le h \le 20$ $-22 \le h \le 22$	$-16 \le h \le 16$ $-17 \le h \le 17$ $-23 \le h \le 22$	$-17 \le h \le 15$ $-23 \le h \le 23$ $-17 \le h \le 19$	$-61 \le h \le 58$ $-23 \le h \le 22$ $-17 \le h \le 17$	$-26 \le h \le 28$ $-21 \le h \le 21$ $-44 \le h \le 46$	$-43 \le \ \le h \le 45$ $-45 \le h \le 45$ $-35 \le h \le 32$	$-20 \le h \le \ \le 13$ $-21 \le h \le 21$ $-34 \le h \le 34$
Reflections collected	6761	29546	28286	53094	59210	78747	80035
Independent reflections	6538 [*R*(int) = 0.0707]	11672 [*R*(int) = 0.0660]	7562[*R*(int) = 0.0829]	12829 [*R*(int) = 0.0915]	14728[*R*(int) = 0.2445]	14792 [*R*(int) = 0.0994]	15411 [*R*(int) = 0.1133]
Completeness to θ	97.3%	90.9%	92.1%	100.0%	100.0%	97.9%	100%
Absorption correction	Empirical	Empirical	Empirical	Empirical	Empirical	Empirical	Empirical
Max. and min. transmission	0.9714 and 0.9549	0.9401 and 0.9200	0.9472 and 0.9253	0.9980 and 0.8303	0.8783 and 0.8195	0.9117 and 0.8186	0.9261 and 0.8190
Refinement method	Full-matrix-least-squares on F^2	Full-matrix-least-squares on F^2	Full-matrix-least-squares on F^2	Full-matrix-least-squares on F^2	Full-matrix-least-squares on F^2	Full-matrix-least-squares on F^2	Full-matrix-least-squares on F^2
Data/restraints/parameters	6538/0/403	11672/0/636	7562/7/473	12829/0/732	14728/7/813	14792/2/763	15411/3/829
Goodness-of-fit	0.832	0.764	1.035	1.050	0.976	0.846	1.152
Final *R* indices [$I > 2\text{sigma}(I)$]	$R1 = 0.0968$, $wR2 = 0.2360$	$R1 = 0.0678$, $wR2 = 0.1897$	$R1 = 0.1317$, $wR2 = 0.2714$	$R1 = 0.0955$, $wR2 = 0.2604$	$R1 = 0.1078$, $wR2 = 0.2719$	$R1 = 0.0560$, $wR2 = 0.1649$	$R1 = 0.1053$, $wR2 = 0.3067$
R indices (all data)	$R1 = 0.2239$, $wR2 = 0.3547$	$R1 = 0.1303$, $wR2 = 0.2440$	$R1 = 0.2095$, $wR2 = 0.3154$	$R1 = 0.1357$, $wR2 = 0.2885$	$R1 = 0.2766$, $wR2 = 0.3249$	$R1 = 0.1117$, $wR2 = 0.1883$	$R1 = 0.1841$, $wR2 = 0.3506$
Largest diff. peak and hole	0.584 and −0.471 e Å^{-3}	0.475 and −0.445 e Å^{-3}	0.503 and −0.309 e Å^{-3}	2.523 and −1.013 e Å^{-3}	1.224 and −0.443 e Å^{-3}	0.873 and −0.470 e Å^{-3}	2.409 and −0.649 e Å^{-3}

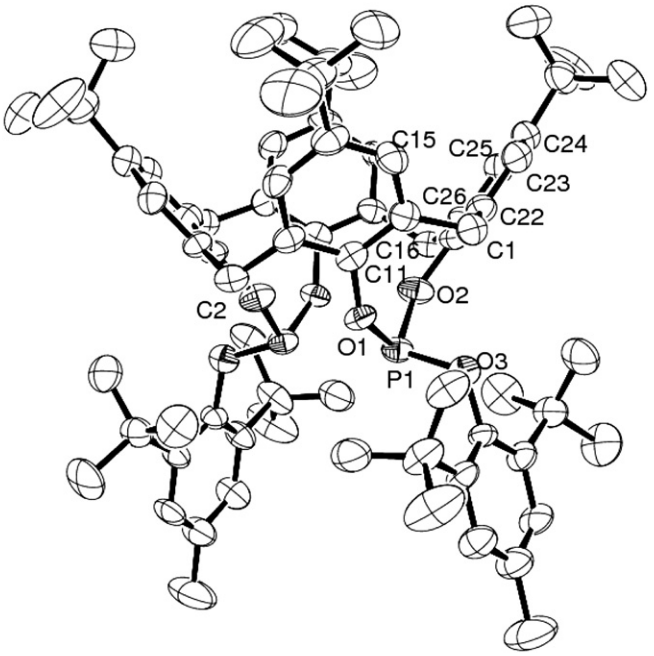

Fig. 2. ORTEP plot of *p-tert*-butyl-calix[4]arene bisphosphite $\mathbf{L}^1$. Thermal ellipsoids are drawn at the 50% probability level. Hydrogen atoms are omitted for clarity.

9a (derived from symmetrically substituted calix[4]arene bisphosphites), **14** and **15** (derived from unsymmetrically substituted calix[4]arene bisphosphites) and cycloplatinated complex **9b** (derived from symmetrically substituted calix[4]arene bisphosphite) as catalysts have been carried out (see Scheme 6). The results are summarized in Table 11. The highest activity was observed when the concentration of the catalysts was 3 mol%. Among all the palladium catalysts, cyclopalladated complex **7** proved to be the best palladium precursor (Table 11 entries 1, 6, 12, 17 and 22) and cyclopalladated complex **8** proved to be a poor palladium precursor (Table 11 entries 2, 8, 13, 18 and 23). The fact that complex **8** shows the lowest activity indicates that the bisphosphite ligand containing *p*-H-calix[4]arene backbone is more π-acidic than the corresponding *p-tert*-butyl derivative and presumably the oxidative-addition step in the catalytic cycle is retarded. Since the palladium centre of cyclopalladated complexes

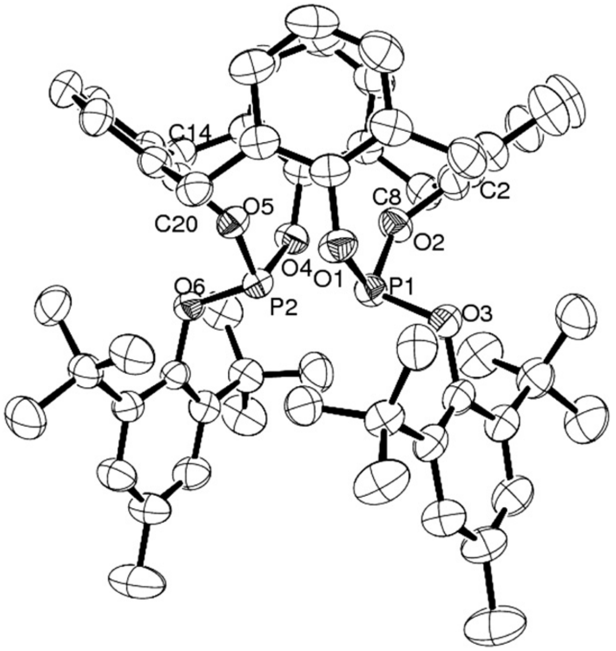

Fig. 3. ORTEP plot of *p-H*-calix[4]arene bisphosphite $\mathbf{L}^2$. Thermal ellipsoids are drawn at the 50% probability level. Hydrogen atoms are omitted for clarity.

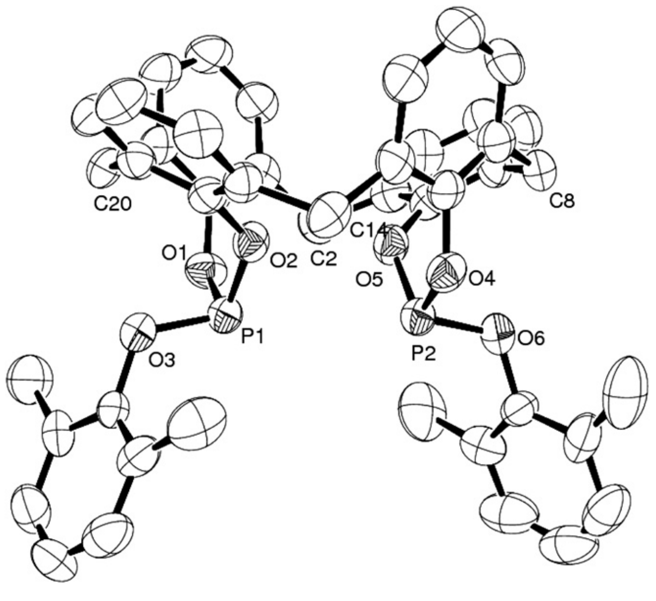

Fig. 4. ORTEP plot of *p-H*-calix[4]arene bisphosphite $\mathbf{L}^6$. Thermal ellipsoids are drawn at the 50% probability level. Hydrogen atoms are omitted for clarity.

Table 4
Selected structural parameters for symmetrically substituted bisphosphites $\mathbf{L}^1$, $\mathbf{L}^2$ and $\mathbf{L}^6$ (distances in Å, angles in °).

	$\mathbf{L}^1$	$\mathbf{L}^2$	$\mathbf{L}^6$
Bond distance			
P(1)–O(1)	1.619 (5)	1.634 (3)	1.628 (5)
P(1)–O(2)	1.608 (5)	1.631 (2)	1.625 (4)
P(1)–O(3)	1.645 (5)	1.652 (2)	1.647 (5)
P(2)–O(4)		1.637 (2)	1.629 (5)
P(2)–O(5)		1.638 (2)	1.623 (5)
P(2)–O(6)		1.649 (2)	1.626 (5)
P(1)···P(2)		3.323 (2)	3.398 (3)
Bond angle			
O(1)–P(1)–O(2)	101.4 (3)	99.61 (1)	99.8 (2)
O(1)–P(1)–O(3)	101.3 (2)	100.59 (1)	102.2 (2)
O(2)–P(1)–O(3)	103.8 (3)	104.34 (1)	100.1 (2)
O(4)–P(2)–O(5)		99.29 (1)	100.0 (2)
O(4)–P(2)–O(6)		100.89 (1)	102.0 (2)
O(5)–P(2)–O(6)		103.77 (1)	99.5 (2)

Table 5
Dihedral angles between the planes[a] of the aryl rings of the calix[4]arene framework and the mean plane (X) defined by the methylene carbon atoms in bisphosphites $\mathbf{L}^1$, $\mathbf{L}^2$ and $\mathbf{L}^6$.

Dihedral angles (°)			
Plane–plane	$\mathbf{L}^1$	$\mathbf{L}^2$	$\mathbf{L}^6$
A–X	51.4 (1)	38.08 (1)	11.67 (2)
B–X	65.4 (1)	81.09 (1)	76.44 (2)
C–X	51.4 (1)	36.40 (1)	11.82 (2)
D–X	65.4 (1)	80.66 (1)	74.07 (2)

[a] A, B, C and D are the planes of aromatic rings defined by C1–C6, C8–C13, C15–C20, C22–C27 for bisphosphite $\mathbf{L}^1$; (C28, C15–C19), (C26, C3–C7), (C1, C21–C25), (C27, C9–C13) respectively for bisphosphites $\mathbf{L}^2$ and $\mathbf{L}^6$.

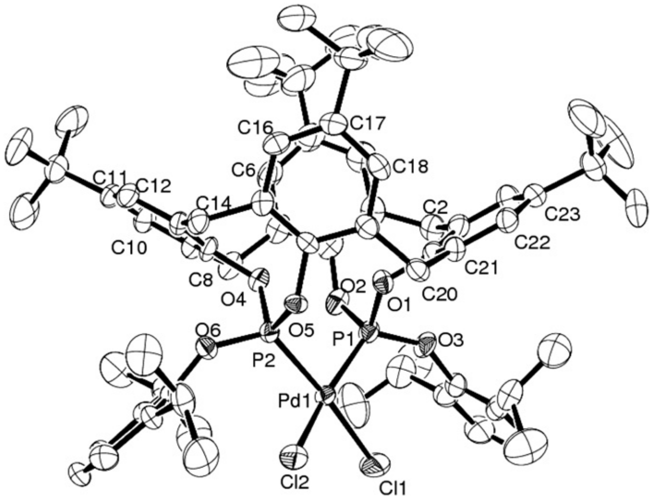

Fig. 5. ORTEP plot of palladium chloride complex **4**. Thermal ellipsoids are drawn at the 50% probability level. Hydrogen atoms are omitted for clarity.

9a, **14** and **15** is more electron rich than that of the cyclopalladated complex **7**, it would be expected that the rate of oxidative-addition would be higher, but the increased electron density at the palladium does not appear to be beneficial. This result suggests that the rate-determining step is probably not oxidative addition but nucleophilic attack of base-activated boronate or reductive elimination of the biaryl product. Hence cyclopalladated complex **7** seems to have about the right balance of electronic and steric properties as catalyst for Suzuki coupling reaction. When the catalyst concentration of **7** was reduced to 1 mol%, the yield of the product decreased (Table 11, entry **7**). The yield of particular biaryl using phenyl chloride as a starting substrate and cyclopalladated complexes **7**, **8**, **9a**, **14** and **15** respectively as catalysts (Table 11, entries 12, 13, 14, 15 and 16), is very poor compared with other aryl halides. Results of comparative studies of the activity of the

Table 6
Selected structural parameters for $PdCl_2$ complexes **4** and **10** (distances in Å, angles in °).

Bond distance	**4**	**10**	Bond angle	**4**	**10**
P(1)–Pd(1)	2.243 (2)	–	P(2)–Pd(1)–P(1)	92.33 (7)	–
P(2)–Pd(1)	2.209 (2)	2.210 (3)	P(2)–Pd(1)–Cl(2)	84.74 (8)	84.14 (1)
Cl(1)–Pd(1)	2.293 (2)	2.323 (4)	P(1)–Pd(1)–Cl(1)	92.17 (9)	–
Cl(2)–Pd(1)	2.334 (2)	2.257 (4)	Cl(2)–Pd(1)–Cl(1)	91.60 (9)	90.72 (2)
P(1)–O(1)	1.590 (6)	1.570 (8)	O(3)–P(1)–O(1)	103.4 (3)	103.3 (4)
P(1)–O(2)	1.595 (6)	1.563 (8)	O(3)–P(1)–O(2)	103.4 (3)	111.7 (4)
P(1)–O(3)	1.565 (5)	1.542 (8)	O(1)–P(1)–O(2)	101.8 (3)	105.5 (4)
P(2)–O(4)	1.593 (5)	–	O(3)–P(1)–Pd(1)	120.1 (2)	–
P(2)–O(5)	1.580 (5)	1.564 (8)	O(1)–P(1)–Pd(1)	105.0 (2)	–
P(2)–O(6)	1.573 (5)	1.575 (8)	O(2)–P(1)–Pd(1)	120.4 (2)	–
O(4)–Pd(1)	–	2.092 (8)	O(6)–P(2)–O(5)	101.4 (3)	101.3 (4)
P(1)–O(4)	–	1.478 (8)	O(6)–P(2)–O(4)	102.7 (3)	–
P(2)–O(7)	–	1.614 (8)	O(5)–P(2)–O(4)	103.3 (3)	–
			O(6)–P(2)–Pd(1)	121.2 (2)	108.9 (3)
			O(5)–P(2)–Pd(1)	112.6 (2)	118.2 (3)
			O(4)–P(2)–Pd(1)	113.6 (2)	–
			O(7)–P(2)–Pd(1)	–	116.6 (3)
			O(4)–Pd(1)–P(2)	–	94.7 (2)
			O(4)–Pd(1)–Cl(1)	–	90.7 (3)
			O(4)–P(1)–O(3)	–	114.0 (4)
			O(4)–P(1)–O(2)	–	111.6 (4)
			O(4)–P(1)–O(1)	–	110.2 (4)

Table 7
Dihedral angles between the planes[a] of the aryl rings of the calix[4]arene framework and the mean plane (X) defined by the methylene carbon atoms in palladium dichloride complexes **4**and **10**.

Dihedral angles (°)		
Plane–plane	**4**	**10**
A–X	83.3 (1)	87.6 (4)
B–X	34.4 (1)	40.7 (3)
C–X	84.8 (2)	79.8 (3)
D–X	29.4 (2)	37.4 (3)

[a] A, B, C and D are the planes of aromatic rings defined by the set of carbon atoms (C28, C15–C19), (C26, C3–C7), (C1, C21–C25), (C27, C9–C13) respectively.

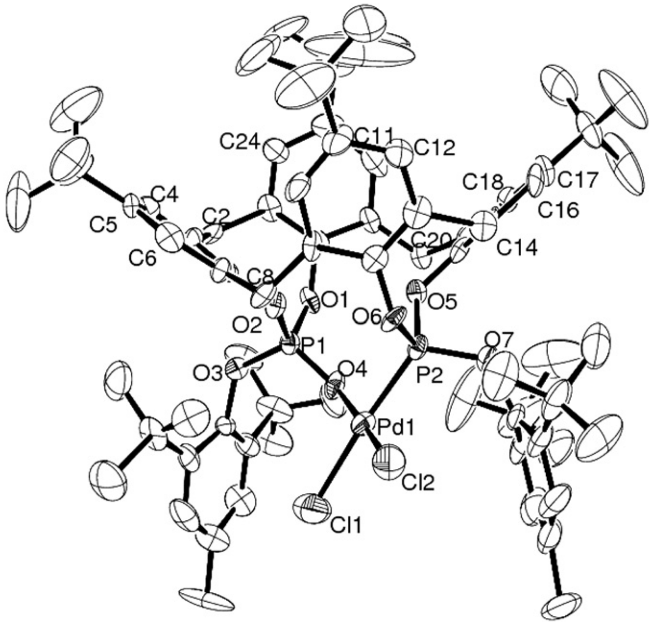

Fig. 6. ORTEP plot of palladium chloride complex **10**. Thermal ellipsoids are drawn at the 50% probability level. Solvent molecules and hydrogen atoms are omitted for clarity.

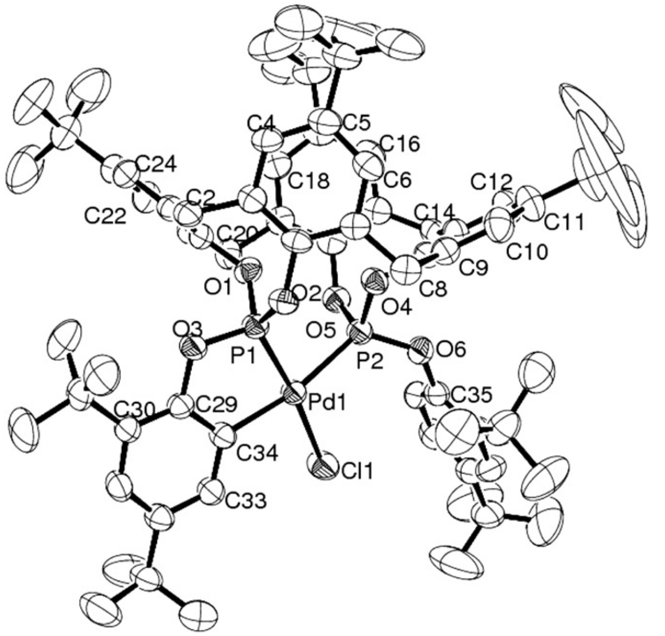

Fig. 7. ORTEP plot of cyclopalladated complex **9a**. Thermal ellipsoids are drawn at the 50% probability level. Hydrogen atoms are omitted for clarity.

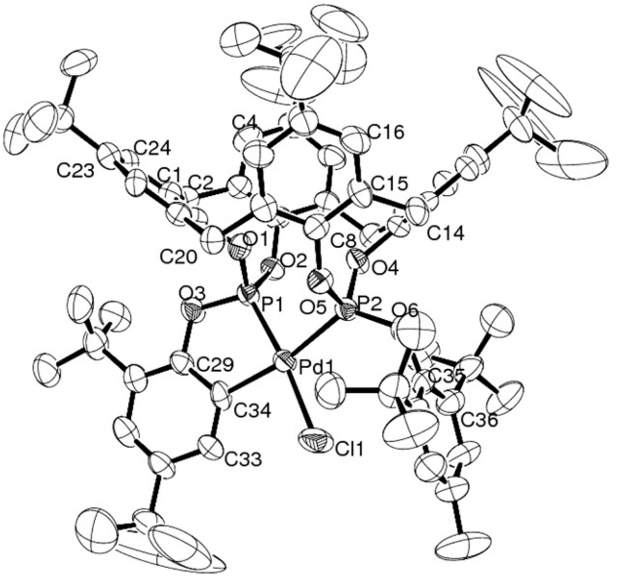

Fig. 8. ORTEP plot of cyclopalladated complex **14**. Thermal ellipsoids are drawn at the 50% probability level. Solvent molecules and hydrogen atoms are omitted for clarity.

cyclopalladated and cycloplatinated complexes **9a** and **9b** in Suzuki coupling of aryl halides (X = H, Me, OMe; Y = I, Br, Cl) with phenyl boronic acid are shown in Table 12. The cycloplatinated complex **9b** proved to be a better catalyst. Overall, the catalytic activities of the cyclometalated complexes (**7**, **8**, **9a**, **9b**, **14**, **15**) in Suzuki coupling reactions are comparable with those reported for other metallacyclic catalysts [17]. Further studies are required to assess the specific beneficial role, if any, of the calixarene framework in catalysis.

3. Experimental

The general experimental procedures and details of spectroscopic measurements are as described in our previous publications [5,10].

3.1. Synthesis of ligands and complexes

The synthetic method reported by Mahalakshmi et al. [5a] for the symmetrically substituted calix[4]arene bisphosphite $\mathbf{L}^1$ was modified to prepare the other symmetrically substituted calix[4]arene bisphosphites ($\mathbf{L}^2$-$\mathbf{L}^6$) by the reaction *p-tert*-butyl-calix[4]arene or *p-H*-calix[4]arene with substituted phenyl phosphorodichloridites, $ROPCl_2$ (R = 2,6-^{t}Bu$_2$–4-Me–C$_6$H$_2$, 2,4-^{t}Bu$_2$–C$_6$H$_3$, 2,6-^{i}Pr$_2$–C$_6$H$_3$ or 2,6-Me–C$_6$H$_3$). The synthesis of unsymmetrically substituted calix[4]arene bisphosphites $\mathbf{L}^7$–$\mathbf{L}^9$ has been described previously [10]. The palladium and platinum dichloride complexes and the cyclometalated complexes (**2**–**15**) were prepared by the reaction of the respective bisphosphite with $PdCl_2(PhCN)_2$, $PdCl_2(COD)$ or $PtCl_2(COD)$. The preparative details and characterization data can be found in Supplementary material.

Table 9
Dihedral angles between the planes[c] of the aryl rings of the calix[4]arene framework and the mean plane (X) defined by the methylene carbon atoms cyclopalladated complexes **9a**, **14** and **7**.

Dihedral angles (°)			
Plane–plane	**9a**	**14**	**7**
A–X	83.0 (1)	71.2 (2)	71.1 (2)
B–X	34.0 (1)	36.4 (2)	37.1 (2)
C–X	81.8 (2)	66.7 (2)	65.7 (2)
D–X	32.5 (1)	41.5 (2)	45.9 (2)

[c] A, B, C and D are the planes of aromatic rings defined (C28, C15–C19), (C26, C3–C7), (C1, C21–C25), (C27, C9–C13) and C1–C6, C8–C13, C15–C16 (Ref. [5a]) for cyclopalladated complexes **9a**, **14** and **7** respectively.

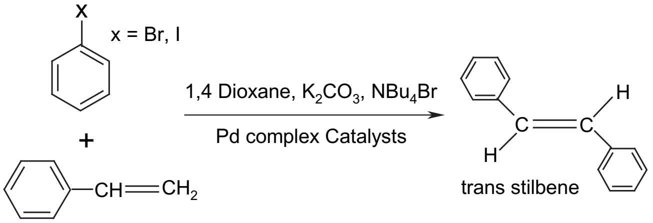

Scheme 5.

3.2. Catalytic studies

The Heck coupling reactions were carried out in a sealed tube at 110° C using K_2CO_3 as the base, 1,4-dioxane as the solvent and NBu_4Br as the co-catalyst under argon atmosphere. Halobenzene (2×10^{-3} mol), styrene (4×10^{-3} mol), K_2CO_3 (3×10^{-3} mol),

Table 8
Selected structural parameters for cyclopalladated complexes **9a**, **14** and **7** (distances in Å, angles in °).[a]

Bond distance	**9a**	**14**	**7**	Bond angle	**9a**	**14**	**7**
P(1)–Pd(1)	2.173 (2)	2.172 (2)	2.165 (2)	P(2)–Pd(1)–P(1)	92.11 (6)	91.15 (8)	91.6 (8)
P(2)–Pd(1)	2.317 (3)	2.334 (2)	2.340 (2)	P(2)–Pd(1)–Cl(1)	93.32 (7)	95.92 (9)	96.4 (8)
Cl(1)–Pd(1)	2.348 (2)	2.315 (3)	2.319 (2)	P(1)–Pd(1)–C(34)	79.7 (1)	81.2 (2)	79.7 (3)
C(34)–Pd(1)	2.070 (5)	2.065 (8)	2.064 (8)	C(34)–Pd(1)–Cl(1)	94.4 (1)	91.6 (2)	92.5 (3)
P(1)–O(1)	1.592 (3)	1.581 (6)	–	O(3)–P(1)–O(1)	102.9 (2)	106.0 (3)	–
P(1)–O(2)	1.578 (3)	1.586 (5)	1.590 (6)	O(3)–P(1)–O(2)	108.5 (2)	103.7 (3)	101.8 (3)
P(1)–O(3)	1.597 (3)	1.606 (6)	1.580 (6)	O(1)–P(1)–O(2)	102.2 (2)	102.4 (3)	–
P(2)–O(4)	1.615 (3)	1.594 (5)	1.590 (5)	O(3)–P(1)–Pd(1)	109.1 (1)	108.5 (2)	110.1 (2)
P(2)–O(5)	1.598 (3)	1.600 (5)	1.592 (6)	O(1)–P(1)–Pd(1)	122.7 (1)	115.0 (2)	–
P(2)–O(6)	1.593 (3)	1.596 (5)	–	O(2)–P(1)–Pd(1)	110.4 (1)	119.9 (2)	121.6(2)
P(1)–O(6)	–	–	1.592 (6)	O(6)–P(2)–O(5)	99.2 (2)	102.9 (3)	–
P(2)–O(1)	–	–	1.602 (6)	O(6)–P(2)–O(4)	106.1 (2)	106.4 (3)	–
				O(5)–P(2)–O(4)	101.9 (2)	101.9 (3)	102.0 (3)
				O(6)–P(2)–Pd(1)	123.3 (1)	125.6 (2)	–
				O(5)–P(2)–Pd(1)	112.2 (1)	109.2 (2)	126.0 (2)
				O(4)–P(2)–Pd(1)	111.5 (1)	108.3 (2)	112.7 (2)

[a] C(34) = C(36) for complex **7**.

Table 10
Results of Heck coupling of aryl halides (X = Br, I) with styrene in presence of cyclopalladated complexes **7**–**9**, **14**, **15**.

Catalyst	Substrate	Base	Time (h)	Yield (%)	TON
7	PhI	K_2CO_3	20	30	3000
8	PhI	K_2CO_3	20	24	2400
9a	PhI	K_2CO_3	20	28	2800
14	PhI	K_2CO_3	20	9	2900
15	PhI	K_2CO_3	20	27	2700
7	PhBr	K_2CO_3	24	24	2400
8	PhBr	K_2CO_3	24	16	1600
9a	PhBr	K_2CO_3	24	18	1800
14	PhBr	K_2CO_3	24	22	2200
15	PhBr	K_2CO_3	24	20	2000

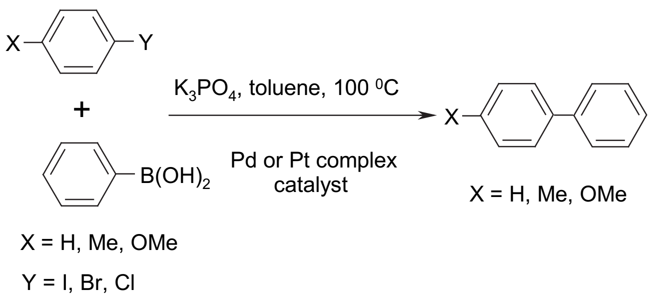

Scheme 6.

cyclometalated palladium complexes (2 mol%) and NBu_4Br (3×10^{-3} mol) in 1,4-dioxane (5 ml) were transferred to a tube (25 ml), fitted with a Teflon cap. The tube was evacuated and flushed with argon gas. The reaction mixture was heated under reflux with stirring at 110 °C for 20–24 h. The reaction mixture was then cooled, solvent evaporated and the residue extracted with diethyl ether to give the crude product, which was purified by column chromatography using petroleum ether/chloroform (100: 5 v/v) as eluant. Each reaction was performed at least twice. The percentage of conversion was calculated on the basis of isolated yields after column chromatographic purification of the product. The product was exclusively trans- stilbene as identified by ^{1}H NMR spectroscopy.

Table 11
Suzuki coupling of aryl halides (X = H, Me, OMe; Y = I, Br, Cl) with phenyl boronic acid in the presence of various cyclopalladated complexes **7**–**9**, **14**, **15**.

Entry	Substrate	Temp.	Time (h)	Base	Catalyst (mol)	Yield (%)	TON
1	C_6H_5I	100 °C	20	K_3PO_4	**7** (0.03)	89	2967
2			20		**8** (0.03)	62	2067
3			20		**9a** (0.03)	80	2667
4			20		**14** (0.03)	84	2800
5			20		**15** (0.03)	78	2600
6	C_6H_5Br	100 °C	20	K_3PO_4	**7** (0.03)	85	2833
7			20		**7** (0.01)	71	7100
8			20		**8** (0.03)	54	1800
9			20		**9a** (0.03)	66	2200
10			20		**14** (0.03)	71	2367
11			20		**15** (0.03)	63	2100
12	C_6H_5Cl	100 °C	24	K_3PO_4	**7** (0.03)	17	567
13			24		**8** (0.03)	7	233
14			24		**9a** (0.03)	15	500
15			24		**14** (0.03)	16	533
16			24		**15** (0.03)	13	433
17	4-Me–C_6H_4Br	100 °C	20	K_3PO_4	**7** (0.03)	68	2267
18			20		**8** (0.03)	42	1400
19			20		**9a** (0.03)	54	1800
20			20		**14** (0.03)	58	1933
21			20		**15** (0.03)	51	1700
22	4-MeO–C_6H_4Br	100 °C	20	K_3PO_4	**7** (0.03)	63	2100
23			20		**8** (0.03)	36	1200
24			20		**9a** (0.03)	47	1567
25			20		**14** (0.03)	54	1800
26			20		**15** (0.03)	47	1567

Table 12
Comparison of the results of Suzuki coupling of aryl halides (X = H, Me, OMe; Y = I, Br, Cl) with phenyl boronic acid in the presence of cyclopalladated complex **9a** and cycloplatinated complex **9b** as catalysts.

Entry	Substrate	Temp.	Time (h)	Base	Catalyst (mol)	Yield (%)	TON
1	C_6H_5I	100 °C	20	K_3PO_4	**9a** (0.03)	80	2672
2			20		**9a** (0.01)	64	6400
3			20		**9a** (0.005)	58	11600
4			20		**9b** (0.03)	88	2933
5			20		**9b** (0.01)	76	7600
6			20		**9b** (0.005)	67	13400
7	C_6H_5Br	100 °C	20	K_3PO_4	**9b** (0.01)	43	4300
8			20		**9b** (0.01)	51	5100
9	C_6H_5Cl	100 °C	24	K_3PO_4	**9a** (0.01)	9	900
10			24		**9b** (0.01)	12	1200
11	4-Me–	100 °C	20	K_3PO_4	**9a** (0.01)	40	4000
12	C_6H_4Br		20		**9b** (0.01)	53	5300
13	4-MeO–	100 °C	20	K_3PO_4	**9a** (0.01)	36	3600
14	C_6H_4Br		20		**9b** (0.01)	47	4700

The Suzuki coupling reactions were carried out using halobenzene or substituted halobenzene, phenyl boronic acid, K_3PO_4 (ratio 1:1.5:2 respectively) and cyclometalated palladium complex or platinum complex (3–0.5 mol%) in toluene (4 ml). The reaction mixture was heated under reflux with stirring at 100 °C for 20–24 h. The reaction mixture was cooled, solvent evaporated and the residue extracted with diethyl ether to give the crude product, which was purified by column chromatography using petroleum ether/chloroform (100: 5 v/v) as eluant. The reactions were performed at least twice and the percentage of conversion was calculated on the basis of isolated yields, after column chromatographic purification of the product. Suzuki coupling product was characterized by ^{1}H NMR spectroscopy by comparing its ^{1}H NMR resonance with that reported for the known compound.

3.3. *X-ray crystallography*

X-ray diffraction data were collected on a Bruker SMART APEX CCD diffractometer. The SMART [18] software was used for cell refinement and data acquisition and the SAINT [19] software used for data reduction. An absorption correction was made on the intensity data using SADABS [20] program. The structures were solved using SHELXS [21] and the WinGX graphical user interface. Least square refinements were performed by the full-matrix method with SHELXL [22]. Some of the *tert*-butyl groups were disordered and hydrogen atoms of these disordered groups were neither located nor fixed during the refinement.

Acknowledgements

We thank the Department of Science and Technology, New Delhi, India for financial support and also for data collection using the CCD X-ray facility at IISc, Bangalore set up under IRHPA program. S.S.K. thanks Indian National Science Academy, New Delhi for a Senior Scientist position.

AppendixA. Supplementary material

CCDC 133304 and 772145-772150 contain the supplementary crystallographic data for symmetrically substituted bisphosphites

(**L**^{1}, **L**^{2} and **L**^{6}), palladium dichloride complexes **4**, **10** and cyclopalladated complexes **9a**, **14**. These data can be obtained free of charge from The Cambridge Crystallographic Data Centre via www.ccdc.cam.ac.uk/data_request/cif.

Appendix. Supplementary material

Supplementary data associated with this article can be found, in the online version, at doi:10.1016/j.jorganchem.2011.06.027.

References

[1] (a) C.D. Gutsche, Calixarenes Revisited. Royal Society of Chemistry, Cambridge, 1998;
(b) L. Mandolini, R. Ungaro, Calixarenes in Action. Imperial College Press, London, 2000.

[2] (a) D.M. Homden, C. Redshaw, Chem. Rev. 108 (2008) 5086;
(b) L. Baldini, A. Casnati, F. Sansone, R. Ungaro, Chem. Soc. Rev. 36 (2007) 254;
(c) S.J. Delgarno, P.K. Thallapallly, L.J. Barbour, J.L. Atwood, Chem. Soc. Rev. 36 (2007) 236;
(d) A. Casnati, F. Sansone, R. Ungaro, Acc. Chem. Res. 36 (2003) 246;
(e) J.T. Lenthall, J.W. Steed, Coord. Chem. Rev. 251 (2007) 1747.

[3] (a) I. Neda, T. Kaukorat, R. Schmutzler, Main Group Chem. News 6 (1998) 4;
(b) C. Kunze, D. Selent, I. Neda, M. Freytag, P.G. Jones, R. Schmutzler, W. Baumann, A. Boner, Z. Anorg. Allg. Chem. 628 (2002) 779;
(c) C. Kunze, D. Selent, I. Neda, R. Schmutzler, A. Spannenberg, A. Boner, Heteroat. Chem. 12 (2001) 577.

[4] (a) C. Jeunesse, D. Armspach, D. Matt, Chem. Commun. 45 (2005) 5603;
(b) C. Jeunesse, C.B. Dieleman, D. Matt, Coord. Chem. Rev. 165 (1997) 93;
(c) C. Jeunesse, C. Dieleman, S. Steyer, D. Matt, J. Chem. Soc., Dalton Trans. (2001) 881;
(d) S. Steyer, C. Jeunesse, J. Harrowfield, D. Matt, Dalton Trans. (2005) 1301;
(e) S. Steyer, C. Jeunesse, D. Matt, R. Welter, M. Wesolek, J. Chem. Soc., Dalton Trans. (2002) 4264;
(f) M. Lejeune, D. Semeril, C. Jeunesse, D. Matt, F. Peruch, P.J. Lutz, L. Ricard, Chem. Eur. J. 10 (2004) 5354;
(g) P. Kuhn, C. Jeunesse, D. Semeril, D. Matt, P. Lutz, R. Welter, Eur. J. Inorg. Chem. (2004) 4602;
(h) D. Semeril, D. Matt, L. Toupet, Chem. Eur. J. 14 (2008) 7144;
(i) C. Jeunesse, C. Dieleman, S. Steyer, D. Matt, J. Chem. Soc. Dalton Trans. (2001) 2508;
(j) D.C. Jeunesse, D. Matt, L. Toupet, Angew. Chem. Int. Ed. 45 (2006) 5810.

[5] (a) L. Mahalakshmi, S.S. Krishnamurthy, M. Nethaji, Curr. Sci. 83 (2002) 870;
(b) A. Sarkar, M. Nethaji, S.S. Krishnamurthy, Polyhedron 26 (2007) 3904;
(c) A. Sarkar, M. Nethaji, S.S. Krishnamurthy, J. Organomet. Chem. 693 (2008) 2097;
(d) A. Sarkar, M. Nethaji, S.S. Krishnamurthy, Tetrahedron 65 (2009) 374;
(e) P. Maji, S.S. Krishnamurthy, M. Nethaji, Polyhedron 27 (17) (2008) 3519;
(f) P. Maji, Inorg. Chim. Acta 372 (2011) 120.

[6] (a) C.J. Cobley, D.D. Ellis, A.G. Orpen, P.G. Pringle, J. Chem. Soc., Dalton Trans. (2000) 1101;
(b) C.J. Cobley, D.D. Ellis, A.G. Orpen, P.G. Pringle, J. Chem. Soc., Dalton Trans. (2000) 1109.

[7] R. Paciello, L. Siggal, M. Roeper, Angew. Chem. Int. Ed. 38 (1999) 1920.

[8] (a) F.J. Parlevliet, M.A. Zuideveld, C. Kiener, H. Kooijman, A.L. Spek, P.C.J. Kamer, P.W.N.M. van Leeuwen, Organometallics 18 (1999) 3394;
(b) F.J. Parlevliet, C. Kiener, J. Franje, K. Goubitz, M. .Lutz, A.N. Spek, P.C.J. Kamer, P.W.N.M. van Leeuwen, J. Chem. Soc., Dalton Trans. (2000) 1113;
(c) A. Marson, Z. Freixa, P.C.J. Kamer, P.W.N.M. van Leeuwen, Eur. J. Inorg. Chem. (2007) 4587;
(d) A. Marson, J. Ernsting, M. .Lutz, A.L. Spek, P.W.N.M. van Leeuwen, P.C.J. Kamer, J. Chem. Soc. Dalton Trans. (2009) 621.

[9] (a) F. Plourde, K. Gilbert, J. Gagnon, P.D. Hervey, Organometallics 22 (2003) 2862;
(b) S. Lai, Q.K.-W. Chan, J. Han, Y.-G. Zhi, N. Zhu, C.-M. Che, Organometallics 28 (2009) 34;
(c) S. Shirakawa, S. Shimuzi, Y. Sasaki, New J. Chem. 25 (2001) 777;
(d) O. Aleksiuk, F. Grynszpan, S.E. Biali, J. Incl. Phenom. Mol. Recogn. 19 (1994) 237.

[10] P. Maji, S.S. Krishnamurthy, M. Nethaji, New J. Chem. 34 (2010) 1478.

[11] (a) R.B. Bedford, C.S.J. Cazin, D. Holder, Coord. Chem. Rev. 248 (2004) 2283;
(b) R.B. Bedford, Chem. Commun. (2003) 1787;
(c) J. Dupont, C.S. Consorti, J. Spencer, Chem. Rev. 105 (2005) 2527;
(d) N. Marion, S.P. Nolan, Acc. Chem. Res. 41 (2008) 1440;
(e) M. Catellani, E. Motti, N.D. Ca, Acc. Chem. Res. 41 (2008) 1512;
(f) I.P. Beletskaya, A.V. Chaeprakov, J. Organomet. Chem. 689 (2004) 4055;
(g) W.A. Herrmann, K. Oefele, D.v. Preysing, S.K. Schneider, J. Organomet. Chem. 687 (2003) 229.

[12] (a) P. He, Y. Lu, Q.-S. Hu, Tetrahedron Lett. 48 (2007) 5283;
(b) R.B. Bedford, L.T. Pilarski, Tetrahedron Lett. 49 (2008) 4216;
(c) R.B. Bedford, M. Betham, J.P.H. Charmant, Mi F. Haddow, A.G. Orpen, L.T. Pilarski, S.J. Coles, M.B. Hursthouse, Organometallics 26 (2007) 6346.

[13] L. Mahalakshmi, Ph.D. Thesis, Synthesis, Structure and Coordination Chemistry of Phosphorus Functionalized Calixarenes, Indian Institute of Science, Bangalore, 1999.

[14] F. Ugozzoli, G.D. Andreetti, J. Incl. Phenom. 13 (1992) 337.

[15] V.V. Dunina, P.A. Zykov, M.V. Livantsov, I.V. Glukhov, K.A. Kochetkov, I.P. Gloriozov, Y.K. Grishin, Organometallics 28 (2009) 425.

[16] (a) Z. Xiong, N. Wang, M. Dai, A. Li, J. Chen, Z. Yang, Org. Lett. 19 (2004) 3337;
(b) D.A. Albisson, R.B. Bedford, P.N. Scully, Tetrahedron Lett. 39 (1998) 9793;
(c) W.A. Herrmann, C. Brossmer, C.-P. Reisinger, T.H. Riermeier, K. Oefele, M. Beller, Chem. Eur. J. 3 (1997) 1357.

[17] (a) W.A. Herrman, V.P.W. Böhm, C.-P. Reisinger, J. Organomet. Chem. 576 (1999) 23;
(b) R.B. Bedford, S.L. Hazelwood, D.A. Albisson, Organometallics 21 (2002) 2599;
(c) R.B. Bedford, C.S.J. Cazin, M.B. Hursthouse, M.E. Light, V.J.M. Scordia, J. Chem. Soc., Dalton Trans. (2004) 3864;
(d) R.B. Bedford, S.L. Welch, Chem. Commun. (2001) 129;
(e) H. Weisserman, D. Milstein, Chem. Commun. (1999) 1901;
(f) B. Rybtchiski, S. Oevers, M. Montag, A. Vigalok, H. Rozenberg, J.M.L. Martin, D. Milstein, J. Am. Chem. Soc. 123 (2001) 9064;
(g) M. Ohff, A. Ohff, M.E. van der Boom, D. Milstein, J. Am. Chem. Soc. 119 (1997) 11687.

[18] Bruker Smart, V. 6.028. Bruker AXS Inc., Madison Wisconsin, USA, 1998.

[19] Bruker Saint, V. 6.02. Bruker AXS Inc., Madison Wisconsin, USA, 1998.

[20] G.M. Sheldrick, SADABS. University of Göttingen, Germany, 1997.

[21] G.M. Sheldrick, SHELXS-97, “Program for Crystal Structure Solution”. University of Göttingen, Göttingen, Germany, 1997.

[22] G.M. Sheldrick, SHELXL-97, “Program for Refinement of Structures”. University of Göttingen, Göttingen, Germany, 1997.